



FORMULATION AND EVALUATION OF FELODIPINE LOADED CHITOSAN NANOPARTICLES

Sunil Kumar Batra*¹ and Dr. Satish Sardana²

¹JJT University, Jhunjhunu, Rajasthan, India.

²Amity Institute of Pharmacy, Amity University, Gurugram, Haryana.

*Corresponding Author: Sunil Kumar Batra
JJT University, Jhunjhunu, Rajasthan, India.
DOI: <https://doi.org/10.17605/OSF.IO/RP6XT>

Article Received on 19/11/2020

Article Revised on 09/12/2020

Article Accepted on 30/12/2020

ABSTRACT

The main objective of the present study was to develop and optimize chitosan nanoparticles of Felodipine by Design of Experiments (DOE). Modified ionic gelation technique was employed for preparation of chitosan nanoparticles due to poor aqueous solubility of Felodipine. The effect of critical formulation variables like, chitosan concentration, TPP concentration, surfactant concentration and process variable like rate of homogenization were studied for the particle size distribution; drug entrapment efficiency and process yield. The dependent variables of the formulations were optimized using 3² full factorial designs and defined in mathematical equations. The desired values of response variables were found by response surface plots and contour plots generated using the design-expert® 10 software. The design was validated by check point analysis. Particle size, drug entrapment efficiency and process yield for the optimized batch were found to be 77.08 nm, 40.63 % and 59.87 % respectively. Thus, using systematic factorial design approach, desired goals can be achieved in shortest possible time with least number of experiments.

KEYWORDS: Chitosan, Design of experiments, Felodipine, Nanoparticles.

INTRODUCTION

Felodipine is a lipophilic crystalline powder and practically insoluble (BCS Class II) in water (solubility: 0.5 mg/l).^[1] The aqueous solubility of a given drug is a very critical factor affecting drug efficacy and safety as it affects drug dissolution parameters and oral bioavailability. For poorly soluble drugs, dissolution step may be the rate limiting process for drug absorption. In addition, poor aqueous solubility and wettability of drug adds to difficulties encountered in drug formulation. As a result, many attempts have been made to improve aqueous solubility of insoluble drugs in order to increase drug efficacy and/or reduce side effects.

Bioavailability of poorly soluble drugs can be improved by various approaches like solubilization, use of cosolvents, salt formation, micronization and complexation with cyclodextrins. One of the excellent methods of improving bioavailability is to make particle size within the nanometric range. Polymeric nanoparticles have diameter less than 1µm and have been used extensively to improve solubility and dissolution rate of poorly soluble drugs.^[2] Selection of polymer for developing nanoparticles largely depends upon desired size of nanoparticles, properties of drug, biocompatibility, toxicity and release profile required.^[3]

Chitosan is the most extensively studied polymer for polymeric nanoparticles.^[4] Due to its low cost, chemical versatility and biodegradability, chitosan is the most popular choice for developing polymeric nanoparticles.^[5] The present study is an attempt to prepare Felodipine loaded chitosan nanoparticles by Design of Experiments (DOE)

MATERIALS AND METHODS

Materials

Felodipine and Chitosan were procured from Yarrow Chemicals, Mumbai, India. All other chemicals were of analytical grade and were purchased from Rankem Lab Reagents, Delhi.

METHODS

Drug polymer compatibility studies

Drug polymer compatibility study is done to assess physical and chemical incompatibility between drug and polymer. Assessment of possible incompatibilities between an active drug substance and polymer was done by DSC and FTIR analysis. FTIR spectra were recorded for Felodipine, chitosan and 1:1 physical mixture of drug and the polymer. DSC study was also performed for same mixtures.

Formulation of nanoparticles of Felodipine

The Felodipine loaded chitosan nanoparticles were prepared by modified ionic gelation of sodium tripolyphosphate (TPP) with chitosan. In this method first O/W emulsion was prepared and then ionic gelation was done by polyanionic molecule as reported by Arjun *et al.*^[6] Chitosan solutions (25 ml) of different concentrations were prepared by dissolving chitosan in 1% acetic acid under stirring at room temperature. After dissolving completely, Tween 80 in different concentrations was added as surfactant. Subsequently Felodipine (50 mg) was dissolved in 2.5 ml of DMSO and then this organic phase was added drop wise to the aqueous phase. This addition was accompanied by high speed stirring (15000, 20000, 25000 rpm) with the help of high speed homogenizer. Stirring was continued for 20 minutes. Sodium tripolyphosphate (TPP) solutions (10 ml) of different concentrations were added drop wise into O/W emulsion under magnetic stirring at 500 rpm in order to induce cross linking of particles. To ensure complete evaporation of organic solvent it was kept overnight at 40° C. Nanoparticles were isolated by centrifugation at 13500 rpm for 20 minutes at 20° C using cooling centrifuge. The pellets were collected and

washed at least three times with double distilled water to remove un-entrapped drugs. Supernatant was used for estimation of free drug. The recovered nanoparticulate suspension was freeze dried using laboratory lyophilizer (Labtech, India).

Experimental Design

Formulation and process variables were optimized using 3² full factorial designs of Design Expert software. Independent critical variables/Factors (X) like chitosan concentration, TPP concentration, surfactant concentration and homogenization speed were optimized. Prepared nanoparticles were characterized and analyzed for mean particle size, drug entrapment efficiency and yield. Critical dependent variables were optimized based on observed responses and analyzed using statistical methods of regression analysis with mathematical equations.

Polymeric particles were prepared using different concentrations of chitosan (0.2 - 0.6% w/v) and TPP (0.2 - 0.6% w/v). The other critical formulation/process variables were kept constant in the composition given in Table 1 below.

Table 1: Composition with different chitosan and TPP concentrations.

Formulation Code	Drug conc (mg)	Chitosan conc (% w/v)	TPP conc (%w/v)	Surfactant conc (% w/v)	Homogenization Speed (rpm)
FN1	50	0.2	0.2	1.5	20000
FN2	50	0.4	0.2	1.5	20000
FN3	50	0.6	0.2	1.5	20000
FN4	50	0.2	0.4	1.5	20000
FN5	50	0.4	0.4	1.5	20000
FN6	50	0.6	0.4	1.5	20000
FN7	50	0.2	0.6	1.5	20000
FN8	50	0.4	0.6	1.5	20000
FN9	50	0.6	0.6	1.5	20000

Now 3 level full factorial design (3²) using Design-Expert® 10 software was used to find out the optimum combination of independent variables (chitosan and TPP

concentration) to obtain desired / response values of dependable variables give in Table 2.

Table 2: Selection of independent and response variables.

3 ² Full Factorial Design				
Factors/Independent Variables		Responses/Dependent variables		
X ₁	X ₂	Y ₁	Y ₂	Y ₃
Chitosan concentration (% w/v)	TPP concentration (% w/v)	Mean particle size (nm)	Drug entrapment efficiency (% w/v)	Process yield (% w/v)

Table 3: Selection of levels for factor/ independent variables.

Levels	Low	Medium	High
Variables	-1	0	+1
Chitosan Concentration (% w/v)	0.2	0.4	0.6
TPP Concentration (% w/v)	0.2	0.4	0.6

Surfactant concentration and homogenization speed

Polymeric nanoparticles were also prepared with different concentrations of surfactant (Tween 80) (1 - 2 % v/v) and homogenization speeds (15000 – 25000 rpm).

The other critical formulation/process variables were kept constant with optimized chitosan and TPP concentration given in following composition (Table 4).

Table 4: Composition with different surfactant concentration and homogenization speed on the basis of experimental design.

Formulation Code	Drug Conc. (mg)	Chitosan Conc (% w/v)	TPP Conc (%w/v)	Surfactant Conc (% v/v)	Homogenization Speed (rpm)
FN10	50	0.4	0.2	1	15000
FN11	50	0.4	0.2	1.5	15000
FN12	50	0.4	0.2	2	15000
FN13	50	0.4	0.2	1	20000
FN14	50	0.4	0.2	1.5	20000
FN15	50	0.4	0.2	2	20000
FN16	50	0.4	0.2	1	25000
FN17	50	0.4	0.2	1.5	25000
FN18	50	0.4	0.2	2	25000

Similarly, full factorial design (3^2) using Design-Expert® 10 software was adopted to find out the optimum combination of factor/ independent variables

(surfactant concentration and homogenization speed) to obtain desired / response values of following dependable variables give in Table 5.

Table 5: Selection of factor variables and response variables.

3 ² Full Factorial Design				
Factors/Independent Variables		Responses/Dependent Variables		
X ₁	X ₂	Y ₁	Y ₂	Y ₃
Surfactant concentration (% v/v)	Homogenization speed (rpm)	Mean particle size (nm)	Drug entrapment efficiency (% w/v)	Yield (% w/v)

Table 6: Selection of levels for factor/independent variables.

Levels	Low	Medium	High
Variables	-1	0	+1
Surfactant Concentration (% v/v)	1	1.5	2
Homogenization Speed (rpm)	15000	20000	25000

Evaluation of nanoparticles

Prepared nanoparticles were evaluated for following parameters.

Yield

Total amount of nanoparticles was weighed individually for each batch and percentage yield was calculated

Practical yield

$$\text{Percentage yield of production} = \frac{\text{Practical yield}}{\text{Theoretical yield}} \times 100 \quad \dots (1)$$

Entrapment efficiency

Amount of Felodipine entrapped in nanoparticles was determined by indirect method. [7] An aliquot of supernatant containing free drug was collected immediately after ultracentrifugation of nanosuspension

taking into consideration weight of drug and polymer Yields of production of different formulations were calculated using the formula.

and analyzed by UV spectroscopy at 361 nm. Entrapment efficiency of Felodipine was calculated according to equation (2)

$$\text{E. E. (\%)} = \frac{\text{Total amount of FDP} - \text{Amount of free FDP}}{\text{Total amount of FDP}} \times 100 \quad \dots (2)$$

Particle size analysis^[8]

Particle size of nanoparticles was determined by dynamic laser scattering technique using Malvern nano S90 (Malvern Instts, UK). Sufficient amount of nanoparticles

was dispersed in double distilled water. Light scattering was measured at 25° and with an angle of 90°.

Zeta potential^[9]

The Zeta potential is the crucial parameter for stability in aqueous nanoparticulate dispersion. It is the electric potential that exists at surface. Zeta potential measures the surface charge of particles. The pellet obtained after centrifugation of nanoparticulate dispersion was redispersed with water. Diluted sample was taken in a cuvet type cell and the zeta potential was measured on a zeta sizer (Malvern Instruments, UK) by determining the electrophoretic mobility. All samples were measured in water at 25^o C in triplicate.

In vitro release^[10]

Optimized batch was also subjected to drug release study. *In vitro* dissolution was performed for Felodipine release study of the nanoparticles in the phosphate buffer pH 6.8 containing 1% Tween 80. Nanoparticles (100 mg) were enclosed in a dialysis memberane 60 (HIMEDIA) and placed into a beaker that contained 900 ml of the dissolution medium. The beaker was placed on a horizontal shaking water bath maintained at 37^oC at a speed of 50 rpm. 5 ml aliquot was withdrawn from the dissolution medium at specific time intervals and analyzed by UV-visible spectrophotometer for Felodipine content at a wavelength of 361 nm. Every time the aliquot was withdrawn from dissolution medium, 5 ml of solution from dissolution medium was added to the vessel in dissolution apparatus to keep its volume constant. All experiments were performed in triplicate. The amount of Felodipine released was calculated by interpolation from a calibration curve containing increasing concentrations of Felodiine.

Dissolution data was presented as cumulated drug released to give the correct picture of the total amount of drug release.

X ray diffraction study

Powder X ray diffraction analysis gives information about crystal lattice arrangements and the degree of crystallinity in the formulation. This study is also useful in identification of physical state of drug.^[9] Powder X ray diffraction spectra was recorded for the pure drug, physical mixture of drug and polymer (1:1) and drug loaded chitosan nanoparticles at room temperature using X ray diffractometer (D₂ PHASER, Bruker, Germany) from 0 to 60 degrees (2 θ) range and a step interval of 0.1 sec.

Transmission electron microscopy (TEM)

Surface morphology of prepared nanoparticles was studied by TEM. A drop of nanosuspension was placed on a carbon film coated copper grid. The copper grid was fixed in to sample holder and placed in a vacuum chamber of transmission electron microscope and observation was made at low vacuum while instrument was operated at 200 kV. TEM images were recorded with a 1k CCD camera.^[11]

RESULTS AND DISCUSSION

Drug polymer compatibility studies

Drug polymer compatibility was studied by the techniques of fourier transform infrared (FTIR) spectroscopy and differential scanning calorimetry (DSC).

FTIR spectroscopy

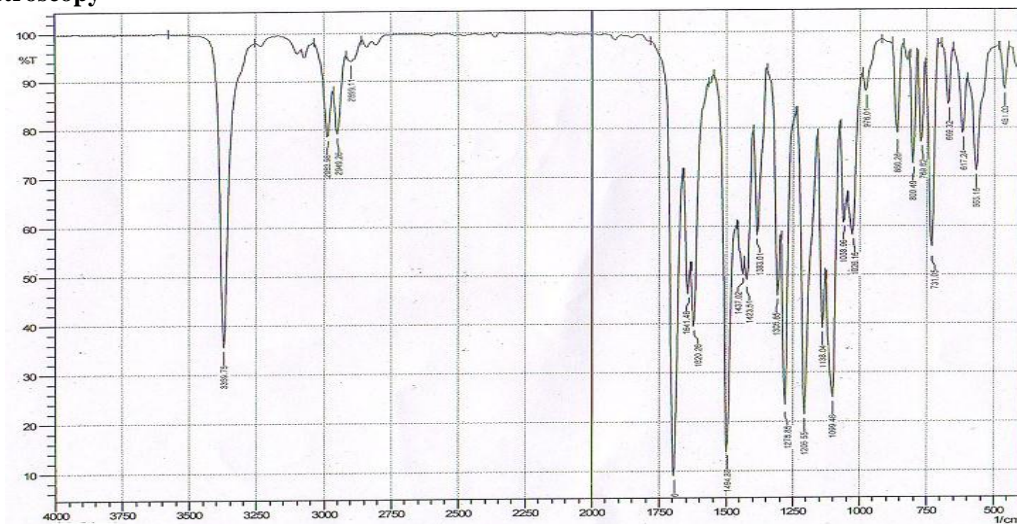


Fig 1: FTIR spectra of Felodipine

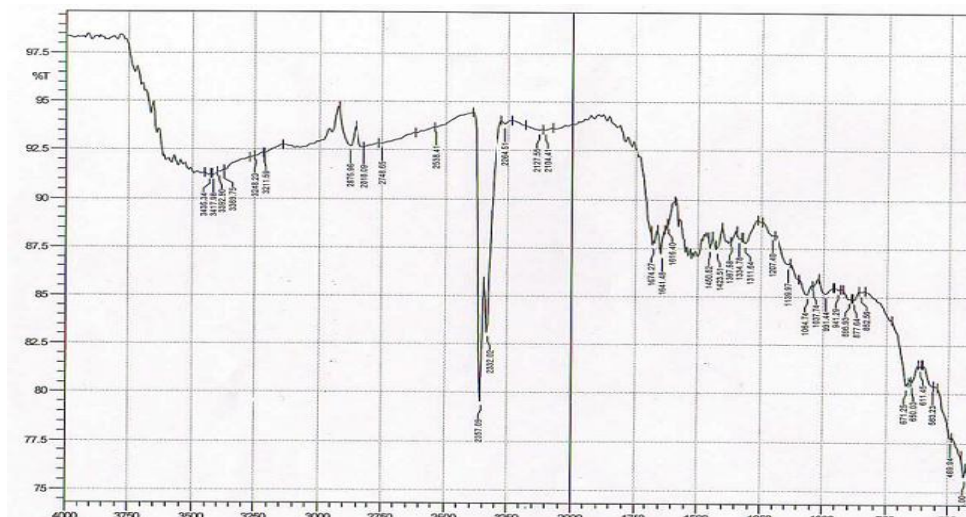


Figure 2: FTIR Spectra of chitosan.

From FTIR spectra of physical mixture of drug and polymer it was observed that all characteristic peaks of Felodipine and chitosan were intact. It shows that there was no incompatibility between the drug and polymer.

FTIR spectrum of Physical mixture of drug and polymer showed characteristic absorption peaks at 3360 (N-H stretching), 2983 (CH stretch, aromatic), 1690 (C=O

stretching), 1495 (C=C ring stretching) and 565 (Cl stretching) cm^{-1} which correspond to Felodipine while peaks at 2837 (CH stretch, aliphatic), 1026 (C-O-C stretching) and 1642 (C=O stretching) cm^{-1} correspond to characteristic peaks of chitosan. From this interpretation it is confirmed that there is no interaction between drug and polymer.

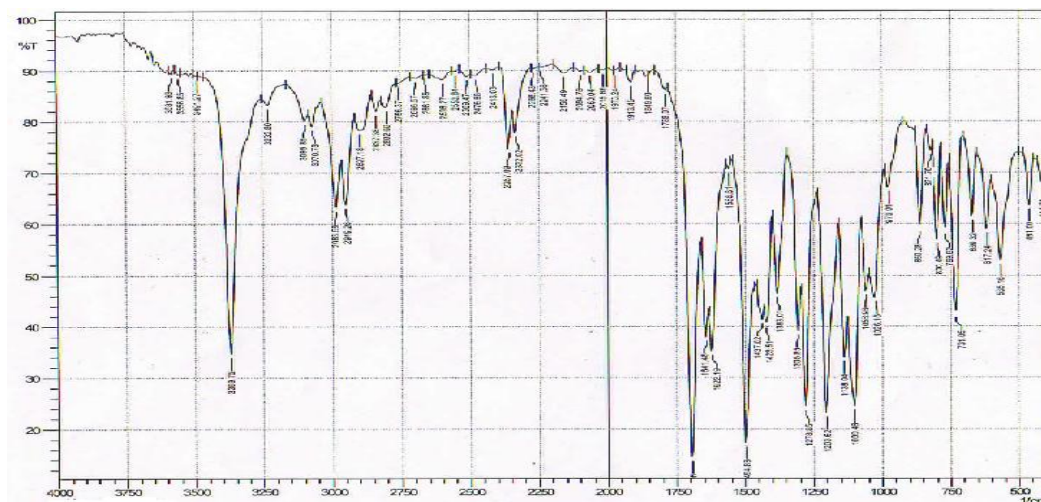


Fig 3: FTIR Spectra of Felodipine and chitosan mixture.

DSC

DSC profile of physical mixture of drug and polymer (1:1) demonstrated retention of Felodipine melting point endotherm at 143° and endothermic peak of chitosan at

its melting point without any additional endothermic peak which proves that there is no incompatibility between the drug and polymer.

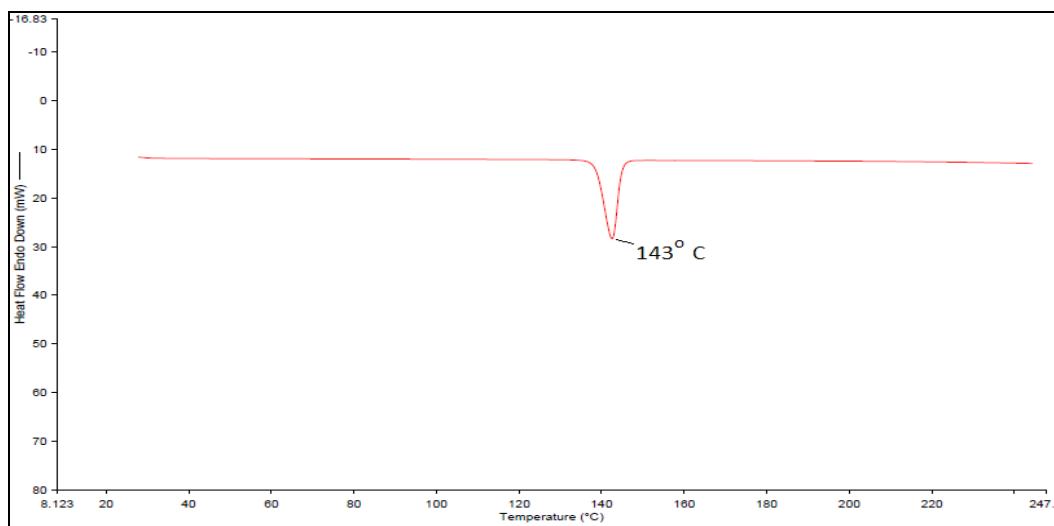


Fig 4.: DSC thermogram of Felodipine.

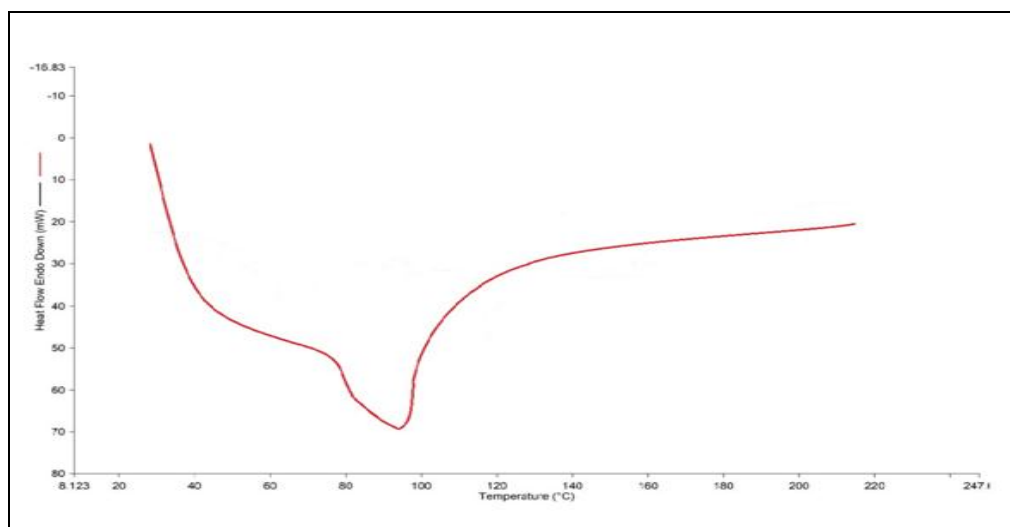


Figure 5: DSC thermogram of chitosan.

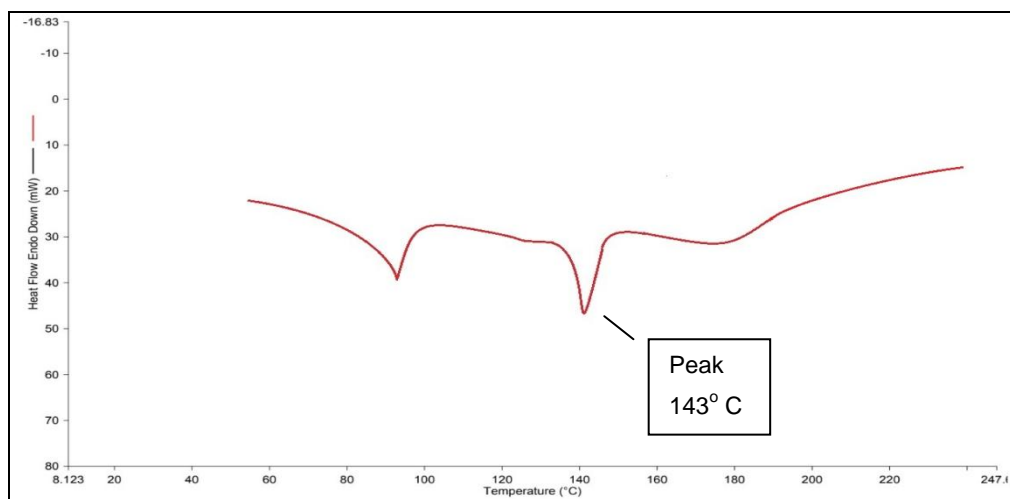


Fig 6: DSC thermogram of Felodipine and chitosan mixture.

Experimental Design

The software had given 9 different runs based on 32 levels for each combination and desired /response values were measured. Design-Expert® 10 software analysed

the two factors (X1 and X2) and measured response surface values (Y1, Y2 and Y3) using appropriate model of ANOVA (Analysis of Variance) for significant value.

Also dependable variables were analysed using 'simple linear regression' to derive mathematical equations.

Statistical analysis of responses by Design Expert 10

Design Expert® version 10 Software (stat Ease Inc. USA) was used for the analysis of effect of each variable on the designated response. The statistical significance of the difference in particle size, percentage of drug entrapment and percent yield was tested by one way analysis of variance (ANOVA) using the following polynomial equation

$$Y = b_0 + b_1X_1 + b_2X_2 + b_3 X_1X_2 + b_4X_1^2 + b_5X_2^2 \dots\dots\dots (3)$$

Where Y is the measured response, b_0 is the arithmetic mean response of all the 9 runs, $b_1 - b_5$ represent estimated coefficients for the factors X_1 and X_2 respectively. The main effects (X_1 and X_2) represent the average result whereas the term X_1X_2 represent the interaction, shows how the response changes when 2 factors are simultaneously changed. The second order terms X_1^2 and X_2^2 indicate the quadratic effect.^[12]

Effect of chitosan and TPP concentration

Effect of chitosan and TPP concentration on various dependent variables is shown below:

Table 7: 3² full factorial design: effect of chitosan and TPP concentration on response variables.

Run	Formula tion Code	Factors/Independent variables		Responses/Dependent variables		
		Chitosan concentration (% w/v) (X_1)	TPP concentration (% w/v) (X_2)	Mean particle size (nm) (Y_1)	Drug entrapment efficiency (% w/w) (Y_2)	Yield (% w/w) (Y_3)
1	FN1	0.2	0.2	108.53	29.26±0.14	42.35±2.21
2	FN2	0.4	0.2	128.2	31.12±1.35	52.43±1.63
3	FN3	0.6	0.2	266.81	34.94±1.76	38.29±0.94
4	FN4	0.2	0.4	148.37	16.26±0.23	47.53±1.37
5	FN5	0.4	0.4	167.42	33.45±1.43	55.63±1.58
6	FN6	0.6	0.4	294.65	27.34±1.33	40.21±0.79
7	FN7	0.2	0.6	195.27	13.57±0.17	49.23±1.18
8	FN8	0.4	0.6	232.43	21.49±0.27	58.47±1.23
9	FN9	0.6	0.6	316.52	25.64±1.84	45.62±0.84

Response 1 – Mean particle size (nm) (Y_1)

Analysis of variance (ANOVA)

Table 8: ANOVA for response surface quadratic model for mean particle size (nm) of nanoparticles.

Source	Sum of Squares	df	Mean Square	F value	p-value Prob>F	
Model	44428.86	5	8885.77	51.55	0.0041	Significant
Chitosan concentration X_1	30219.03	1	30219.03	175.32	0.0009	
TPP Concentration X_2	9654.48	1	9654.48	56.01	0.0049	
$X_1 * X_2$	342.81	1	342.81	1.99	0.2533	
X_1^2	4172.41	1	4172.41	24.21	0.0161	
X_2^2	40.14	1	40.14	0.2329	0.6624	

Regression analysis

Table 9: Regression analysis with regular model for mean particle size (nm) of nanoparticles.

Details	Coefficients	Standard Error	df	Lower 95% CI	Upper 95% CI
Intercept	173.03	9.79	1	141.89	204.17
Chitosan concentration X_1	70.97	5.36	1	53.91	88.03
TPP Concentration X_2	40.11	5.36	1	23.06	57.17
$X_1 * X_2$	-9.26	6.56	1	-30.15	11.63
X_1^2	45.67	9.28	1	16.13	75.22
X_2^2	4.48	9.28	1	-25.06	34.02

Table 10: Regression analysis with reduced model for mean particle size (nm) of nanoparticles.

Details	Coefficients	Standard Error	Df	Lower 95% CI	Upper 95% CI
Intercept	176.02	7.75	1	156.10	195.93
Chitosan concentration X_1	70.97	5.48	1	56.89	85.05
TPP Concentration X_2	40.11	5.48	1	26.03	54.19
X_1^2	45.67	9.49	1	21.29	70.06

Response 1 - Mean particle size (Y_1): Values of particle size of all the 9 batches showed variation from 108.53 nm to 316.52 nm. Particle size increased dramatically with increasing concentration of both chitosan and TPP but amongst them effect of chitosan concentration was more significant than TPP. Increase in particle size with increase in chitosan concentration is due to the fact that at higher concentration of chitosan, viscosity is much higher and hence it affects shear capacity of homogenizer and stirrer. When concentration of chitosan is low, it forms a low viscosity gelation medium resulting in decrease in liquid phase dispersion, thus promoting formation of small particles. Particle size increases with increase in concentration of TPP due to stiffness of crosslinkage between TPP and chitosan. As TPP concentration increases, there would be more tripolyphosphoric ions to cross-link with amino group on chitosan chains.^[13] Minimum particle size (108.53 nm) was obtained with FN1 batch with drug entrapment efficiency of 29.26% and production yield of 42.35%.

The software analysed the ANOVA for response surface with Quadratic model. The Model F-value of 51.55 indicates the model was significant. There was only a 0.41 percent chance that a "Model F-Value" this large could occur due to noise. P values of less than 0.0500 indicate model terms were significant. In this case, X_1 , X_2 and X_1^2 were significant model terms given in Table 8.

Regression analysis: The effect of independent variables was evaluated using simple linear regression analysis given in Table 9. The process data was evaluated at 95% confidence interval with regular model. The process data of reduced model given in Table 10 indicated that mean particle size (Y_1) depends upon variation in chitosan concentration (X_1), TPP

concentration (X_2) and square of chitosan concentration (X_1^2) and it is defined by following equation.

Mean particle size (nm) (Y_1) = intercept + coefficient * X_1 + coefficient * X_2 + coefficient * X_1^2
 $= +176.02 + 70.97 * X_1 + 40.11 * X_2 + 45.67 * X_1^2$ (4)

The regression statistics provided Multiple R 0.9771 and 0.9604; R Square 0.9885 and 0.9800 for regular and reduced model respectively. The **3D surface graph** between chitosan concentration and TPP concentration indicated lower mean particle size in nm obtained with decrease in both chitosan concentration and TPP concentrations. The effect was more significant with chitosan as shown in Figure 7.

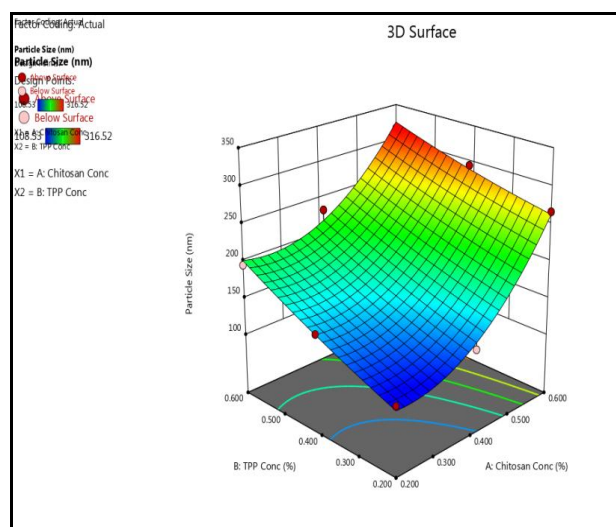


Figure 7: 3D surface graph for mean particle size (nm) of nanoparticles using different concentrations of chitosan and TPP.

Response 2 – Percent drug entrapment efficiency (Y_2) Analysis of variance (ANOVA)

Table 11: ANOVA for response surface quadratic model for % drug entrapment efficiency of nanoparticles.

Source	Sum of Squares	Df	Mean Square	F value	p-value Prob>F	
Model	338.29	2	169.14	9.62	0.0134	Significant
Chitosan concentration X_1	138.53	1	138.53	7.88	0.0309	
TPP Concentration X_2	199.76	1	199.76	11.36	0.0150	

Regression analysis.

Table 12: Regression analysis with regular model for % drug entrapment efficiency of nanoparticles.

Details	Coefficients	Standard Error	df	Lower 95% CI	Upper 95% CI
Intercept	25.90	1.40	1	22.48	29.32
Chitosan concentration X ₁	4.81	1.71	1	0.6157	8.99
TPP Concentration X ₂	-5.77	1.71	1	-9.96	-1.58

Response 2 – Percent drug entrapment efficiency (Y₂):

Drug entrapment of the 9 formulations varied from 13.57% to 34.94%. It was observed that entrapment efficiency increased from 29.26 to 34.94, from 16.26 to 27.34 and 13.57 to 25.64 with increase in concentration of chitosan with respect to amount of drug at different concentrations of TPP. Entrapment efficiency is more when there is increase in chitosan concentration because higher amount of chitosan tend to have higher ability of ionic gel formation which prevents drug movement to external phase and results in increase in drug entrapment efficiency. As has been observed that particle size increases with increase in concentration of chitosan, more material and bigger particles could encapsulate more drug. Maximum drug entrapment was obtained for FN3 batch prepared with highest concentration of chitosan and lowest concentration of TPP but the process yield and particle size obtained were 38.29% and 266.81

nm respectively which was beyond desired goal. The software analysed the ANOVA for response surface with Linear model. The Model F-value of 9.62 indicates the model was significant. There was only a 1.34 percent chance that a "Model F-Value" this large could occur due to noise. P values of less than 0.0500 indicate model terms were significant. In this case, X₁, and X₂ were significant model terms given in Table 11.

Regression analysis: The effect of independent variables was evaluated using simple linear regression analysis given in Table 12. The process data was evaluated at 95% confidence interval with regular model. The process data of regular model indicated that percent entrapment efficiency (Y₂) depends upon variation in chitosan concentration (X₁) and TPP concentration (X₂). It is defined by following equation:.

Percent entrapment efficiency (Y₂) = intercept + coefficient * X₁ - coefficient * X₂
 = + 25.90 + 4.81 * X₁ - 5.77 * X₂ (5)

The regression statistics provided Multiple R 0.5809 and R Square 0.7622 for regular model.

efficiency (30-40%) can be obtained with higher polymer concentration (approx 0.4 to 0.6 % w/v) at minimum concentration range of TPP shown in Figure 8.

The **3D surface graph** between polymer and drug concentration indicated higher drug entrapment

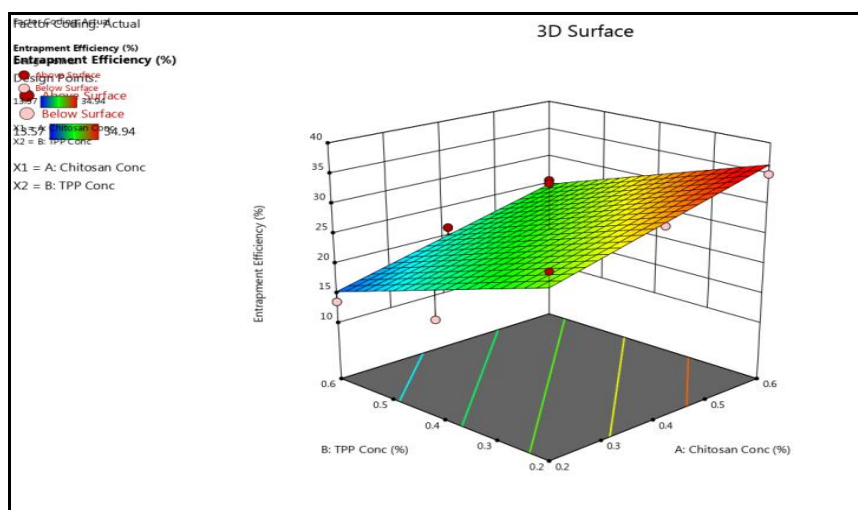


Figure 8: 3D surface graph for drug entrapment efficiency of nanoparticles using different concentrations of chitosan and TPP.

Response 3 – Yield (Percent) (Y₃)**Analysis of variance (ANOVA)****Table 13: ANOVA for response surface quadratic model for % yield of nanoparticles.**

Source	Sum of Squares	df	Mean Square	F value	p-value Prob>F	
Model	376.75	5	75.35	50.90	0.0042	Significant
Chitosan concentration X ₁	37.45	1	37.45	25.30	0.0151	
TPP concentration X ₂	68.34	1	68.34	46.16	0.0065	
X ₁ *X ₂	0.0506	1	0.0506	0.0342	0.8651	
X ₁ ²	270.90	1	270.90	182.99	0.0009	
X ₂ ²	0.0068	1	0.0068	0.0046	0.9502	

Regression analysis**Table 14: Regression analysis with regular model for % yield of nanoparticles.**

Details	Coefficients	Standard Error	df	Lower 95% CI	Upper 95% CI
Intercept	55.55	0.9069	1	52.66	58.44
Chitosan concentration X ₁	-2.50	0.4967	1	-4.08	-0.9175
TPP Concentration X ₂	3.37	0.4967	1	1.79	4.96
X ₁ *X ₂	0.11125	0.6084	1	-1.82	2.05
X ₁ ²	-11.64	0.8604	1	-14.38	-8.90
X ₂ ²	-0.0583	0.8604	1	-2.80	2.68

Table 15: Regression analysis with reduced model for % yield of nanoparticles.

Details	Coefficients	Standard Error	Df	Lower 95% CI	Upper 95% CI
Intercept	55.51	0.5476	1	54.10	56.92
Chitosan concentration X ₁	-2.50	0.3872	1	-3.49	-1.50
TPP Concentration X ₂	3.37	0.3872	1	2.38	4.37
X ₁ ²	-11.64	0.6707	1	-13.36	-9.91

Response -3: Percent yield (Y₃)

Percent practical yield of the 9 formulations varied from 38.29% to 58.47 %. Practical yield tended to increase with increase in concentration of chitosan but only up to 0.4% concentration, beyond that percent yield decreased significantly. It was observed that percent yield increased with increase in concentration of TPP but the effect was not very significant. Maximum practical yield was obtained with FN8 batch prepared with 0.4% concentration of chitosan and 0.6 % concentration of TPP but the particle size and entrapment efficiency obtained were 232.43 nm and 21.49 % respectively which was beyond desired goal.

The software analysed the ANOVA for response surface with Quadratic model. The Model F-value of 50.90

indicates the model was significant. There was very little chance (0.42 percent) that this much "Model F-Value" could occur due to noise. P values of less than 0.0500 indicate model terms were significant. In this case, X₁, X₂ and X₁² were significant model terms as given in Table 13.

Regression analysis: The effect of independent variables was evaluated using simple linear regression analysis given in Table 14. The process data was evaluated at 95% confidence interval with regular model. The process data of reduced model given in Table 15 indicated that percentage yield (Y₃) depends upon variation in chitosan concentration (X₁), TPP concentration (X₂) and square of chitosan concentration (X₁²) It is defined by following equation.

$$\text{Process yield (Y}_3\text{)} = \text{intercept} - \text{coefficient} * X_1 + \text{coefficient} * X_2 - \text{coefficient} * (X_1)^2$$

$$= + 55.51 - 2.50 * X_1 + 3.37 * X_2 - 11.64 * X_1^2 \quad \dots\dots\dots (6)$$

The regression statistics provided Multiple R 0.9767 and 0.9765; R Square 0.9883 and 0.9882 for regular and reduced model respectively. The **3D surface graph** between chitosan concentration and TPP concentration

(Figure 9) indicated that higher practical yield can be obtained with chitosan concentration of 0.4 %. TPP concentration though has a positive effect on percentage yield but effect was not very significant.

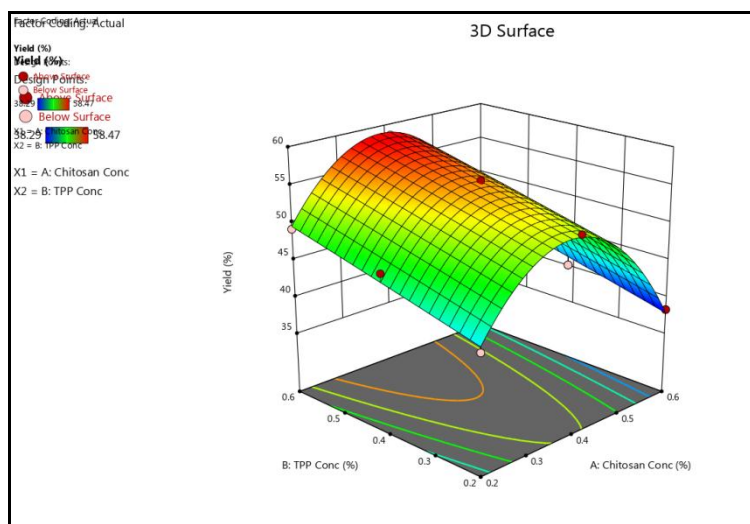


Figure 9: 3D surface graph for percent yield of nanoparticles using different of chitosan and TPP concentrations.

Optimization Graph

The contour overlay graph (Figure 10) for optimum desired value (yellow shaded region) gave variety of combinations to get better drug entrapment efficiency, better percent yield and narrow particle size range. Based

on peak value, 0.4% w/v chitosan and 0.2% w/v TPP were considered optimum concentrations to give mean particle size <(120 nm), percent drug entrapment efficiency~(30-40%) and percent yield~(50-60%).

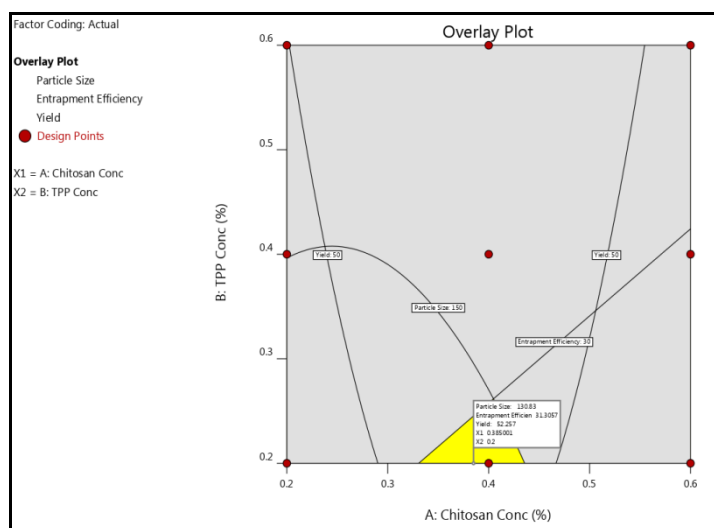


Figure 10: Contour overlay graph for optimum desired response variables for different chitosan and TPP concentration.

Further, surfactant concentration and homogenization speed were optimized to get desired mean particle size and its distribution; percent yield and percent drug entrapment efficiency.

and homogenization speed was studied on various evaluation parameters.

Effect of surfactant concentration and homogenization speed

Polymeric nanoparticles were prepared with different concentrations of surfactant (Tween 80) (1 -2 % v/v) and homogenization speeds (15000 – 25000 rpm). The other critical formulation/process variables were kept constant with optimized chitosan and TPP concentration given in composition Table 3.6. Effect of surfactant concentration

Table 16: 3² full factorial design: effect of surfactant concentration and homogenization speed on response variables.

Run	Batch	Factors/Independent variables		Responses/dependent variables		
		Surfactant concentration (% v/v) (X ₁)	Homogenization Speed (rpm) (X ₂)	Mean particle size (nm) (Y ₁)	Drug entrapment efficiency (% w/w) (Y ₂)	Yield (% w/w) (Y ₃)
1	FN10	1	15000	218.93	24.87±1.67	42.12±2.52
2	FN11	1.5	15000	190.35	26.54±1.43	44.72±1.94
3	FN12	2	15000	160.12	28.95±1.17	47.36±1.25
4	Fn13	1	20000	136.66	29.76±0.98	49.41±1.04
5	FN14	1.5	20000	129.42	32.14±1.05	51.67±1.15
6	FN15	2	20000	122.24	36.56±1.22	54.86±0.82
7	FN16	1	25000	118.63	37.74±0.64	55.15±0.88
8	FN17	1.5	25000	98.52	38.57±0.53	57.29±0.62
9	FN18	2	25000	84.70	39.23±0.58	59.45±0.47

Response 1 – Mean particle size (nm) (Y₁)**Table 17: ANOVA for response surface quadratic model for mean particle size (nm) of nanoparticles.**

Source	Sum of Squares	df	Mean Square	F value	p-value Prob>F	
Model	13844.38	2	6922.59	41.56	0.0003	Significant
Surfactant concentration X ₁	1913.88	1	1913.88	11.49	0.0147	
Homogenization speed X ₂	11930.50	1	11930.50	71.63	0.0001	

Regression analysis**Table 18: Regression analysis with regular model for mean particle size (nm) of nanoparticles.**

Details	Coefficients	Standard Error	Df	Lower 95% CI	Upper 95% CI
Intercept	139.95	4.30	1	129.43	150.48
Surfactant concentration X ₁	-17.86	5.27	1	-30.75	-4.97
Homogenization speed X ₂	-44.59	5.27	1	-57.48	-31.70

Response -1: Mean particle size (Y₁)

Particle size is an important parameter because it has a great relevance to stability of formulation. Large particles tend to aggregate to a great extent compared to smaller particles. It was observed that as surfactant concentration (X₁) increased from 1 % to 2 % v/v, the mean particle size was also decreased in trend, but not significantly from 218.93 nm to 160.12 nm; 136.66 nm to 122.24 nm and 118.63 nm to 84.7 nm at different homogenization speed (X₂) of 15000 rpm, 20000 rpm and 25000 rpm respectively. It was also observed that as homogenization speed (X₂) increased from 15000 rpm to 25000 rpm, the mean particle size decreased significantly as indicated in trend, at different emulsifier concentration (1-2% v/v). The result indicated that significant decreases in mean particle size (118.63 nm-84.7 nm) were found at 25000 rpm homogenization speed (X₂) with different emulsifier concentration (1-2% v/v). It can be well explained when surfactant and homogenization speed increased, the internal phase containing polymer and drug was stabilized into smaller particles, as DMSO evaporates slowly during continuous mixing. The higher emulsifier concentration reduced the total surface tension at the interface of droplets, hence droplets were sub divided in the continuous phase and stabilized slowly as DMSO evaporates out. At high

homogenization speed (25000 rpm), total internal dynamic energy also increased, resulting in decrease in droplet size of internal phase significantly. Since internal phase contain higher 0.4% w/v polymer and 50 mg drug could stabilized in the particle size range (84.70 - 118.63 nm) and encapsulate drug at optimum level with narrow standard deviation. Therefore, the result indicated that there is directly inversely proportional relationship between emulsifier concentration and homogenization speed to the mean particle size and size distribution of nanoparticles given in Table 7 and 16.

The software analysed the ANOVA for response surface with Linear model. The **Model F-value** of 41.56 indicates the model was significant. There was very less chance (0.03 percent) that this much "Model F-Value" could occur due to noise. The values of "Prob > F" were less than 0.0500 which implies that the model terms were significant. In this case X₁ and X₂ were significant model terms as given in Table 17.

Regression analysis: The effect of independent variables was evaluated using simple linear regression analysis given in Table 18. The process data was evaluated at 95% confidence interval with regular model. The process data of regular model indicated that mean

particle size (Y_1) linearly depends upon variation in surfactant concentration (X_1) and homogenization speed

(X_2), it is defined by following equation,

$$\text{Mean particle size (nm)} (Y_1) = \text{intercept} - \text{coefficient} * X_1 - \text{coefficient} * X_2$$

$$= + 139.95 - 17.86 * X_1 - 44.59 * X_2 \dots\dots\dots (7)$$

The regression statistics provided Multiple R 0.8699 and R Square 0.9327 for regular model. The **3D surface graph** between surfactant concentration and homogenization speed indicated lower mean particle size in nm obtained with increase in homogenization speed at

different 1-2% w/v emulsifier concentration range. Hence effect of homogenization speed on particle size distribution was more significant than emulsifier concentration as shown in Figure 11.

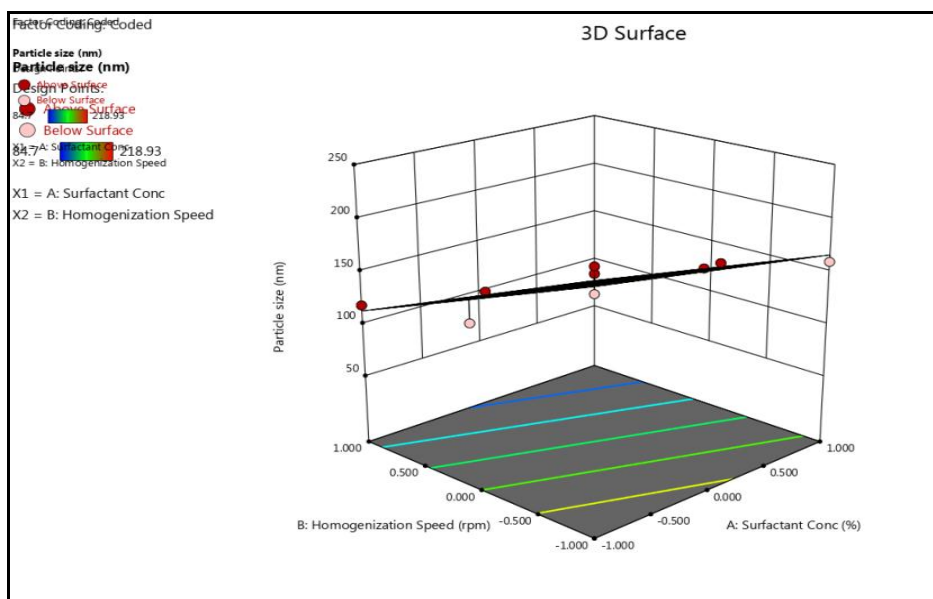


Figure 11: 3D surface graph for mean particle size (nm) of FDP nanoparticles using different surfactant concentration and homogenization speed.

Response 2 – Drug entrapment efficiency (Percent) (Y_2)

Table 19: ANOVA for response surface linear model for % drug entrapment efficiency of nanoparticles.

Source	Sum of Squares	df	Mean Square	F value	p-value Prob>F	
Model	231.77	2	98.85	88.04	<0.0001	Significant
Surfactant concentration X_1	25.50	1	25.50	19.37	0.0046	
Homogenization speed X_2	206.27	1	206.27	156.70	<0.0001	

Regression analysis

Table 20: Regression analysis with regular model for % drug entrapment efficiency of nanoparticles.

Details	Coefficients	Standard Error	Df	Lower 95% CI	Upper 95% CI
Intercept	32.71	0.3824	1	31.77	33.64
Surfactant concentration X_1	2.06	0.4684	1	0.9156	3.21
Homogenization speed X_2	5.86	0.4684	1	4.72	7.01

Response -2: Percent drug entrapment efficiency (Y_2)
 Drug entrapment of the 9 formulations varied from 24.87% to 39.23%. Entrapment efficiency tended to increase with increase in Homogenization speed. It can be explained as emulsifier quantity and homogenization speed increased, droplets size of the internal phase in emulsion reduced due to reduction of interfacial surface tension at interface, hence total surface area of internal phase increased. The small sized droplets contained drug

and polymer which was well stabilized through nano sized emulsion, hence the encapsulation of drug within polymer increased significantly. Therefore it was evident that percent drug entrapment increased from 24.87 to 39.23% as emulsifier quantity and homogenization speed increased. Hence, the result indicated that there is directly proportion relationship between emulsifier concentration and homogenization speed to the percent

drug entrapment efficiency of nanoparticles given in Table 7 and 16.

The software analysed the ANOVA for response surface with Linear model. The Model F-value of 88.04 indicates the model was significant. There was very less chance (0.01 percent) chance that this much "Model F-Value" could occur due to noise. P values of less than 0.0500 indicate model terms were significant. In this case, X₁, and X₂ were significant model terms. as given in Table 19.

Regression analysis: The effect of independent variables was evaluated using simple linear regression analysis given in Table 20. The process data was evaluated at 95% confidence interval with regular model. The process data of regular model indicated that percent entrapment efficiency (Y₂) depends upon variation in surfactant concentration (X₁) and homogenization speed (X₂), it is defined by following equation.

$$\text{Drug entrapment efficiency (\%)} (Y_2) = \text{intercept} + \text{coefficient} * X_1 + \text{coefficient} * X_2 \\ = + 32.71 + 2.06 * X_1 + 5.86 * X_2 \dots\dots\dots (8)$$

The regression statistics provided Multiple R 0.9351 and R Square 0.9670 for regular model The **3D surface graph** between surfactant concentration and

homogenization speed indicated drug entrapment efficiency obtained with shown in Figure 12.

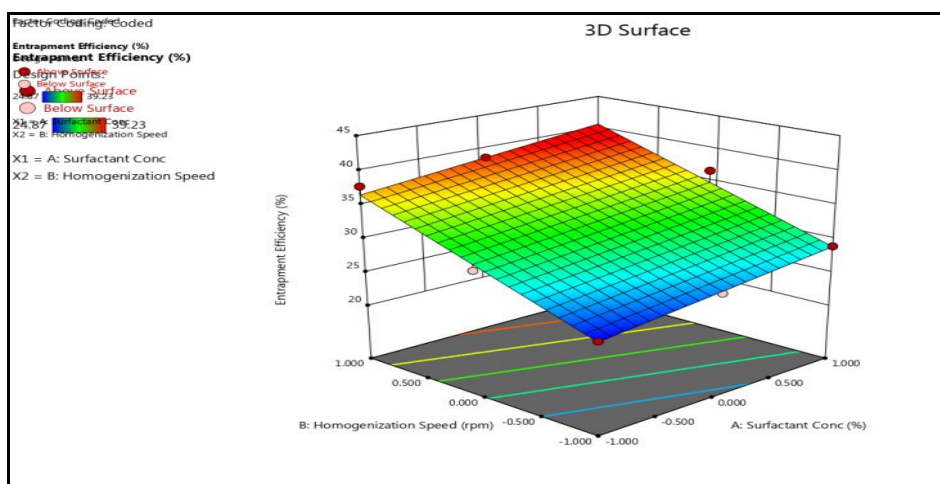


Figure 12: 3D surface graph for drug entrapment efficiency of nanoparticles using different surfactant concentration and homogenization speed.

Response 3 – Yield (Percent) (Y₃)

Table 21: ANOVA for response surface quadratic model for % yield of Felodipine loaded chitosan nanoparticles.

Source	Sum of Squares	df	Mean Square	F value	p-value Prob>F	
Model	276.34	5	55.27	679.07	<0.0001	Significant
Surfactant concentration X ₁	37.45	1	37.45	460.14	0.0002	
Homogenization speed X ₂	236.76	1	236.76	2908.95	<0.0001	
X ₁ *X ₂	0.2209	1	0.2209	2.71	0.1980	
X ₁ ²	0.0544	1	0.0544	0.6690	0.4733	
X ₂ ²	1.86	1	1.86	22.88	0.0174	

Regression analysis

Table 22: Regression analysis with regular model for % yield of nanoparticles.

Details	Coefficients	Standard Error	Df	Lower 95% CI	Upper 95% CI
Intercept	51.87	0.2126	1	51.19	52.55
Surfactant concentration X ₁	2.50	0.1165	1	2.13	2.87
Homogenization speed X ₂	6.28	0.1165	1	5.91	6.65
X ₁ *X ₂	-0.2350	0.1426	1	-0.6890	0.2190
X ₁ ²	0.1650	0.2017	1	-0.4770	0.8070
X ₂ ²	-0.9650	0.2017	1	-1.61	-0.3230

Table 23: Regression analysis with reduced model for % yield of nanoparticles.

Details	Coefficients	Standard Error	Df	Lower 95% CI	Upper 95% CI
Intercept	51.98	0.1861	1	51.50	52.46
Surfactant concentration X ₁	2.50	0.1316	1	2.16	2.84
Homogenization speed X ₂	6.28	0.1316	1	5.94	6.62
X ₂ ²	-0.9650	0.2279	1	-1.55	-0.3791

Response -3: Percent yield (Y₃)

Percent process yield for all formulations varied from 42.12 % to 59.45 %. It was observed that process yield increased with increase in homogenization speed at different surfactant concentrations. When homogenization speed (X₂) was increased from 15000 rpm to 25000 rpm, the process yield increased up to 55.15 - 59.45 %, from 42.12 – 47.36 % for different surfactant concentration (X₁) levels 1-2 %.

The software analysed the ANOVA for response surface with Quadratic model. The Model F-value of 679.07 indicates the model was significant. There was very little chance (0.01 percent) that this much "Model F-Value" could occur due to noise. P values of less than 0.0500

Percent process yield (Y₃) = intercept + coefficient*X₁ + coefficient*X₂ – coefficient*(X₂)²
= + 51.98 + 2.50*X₁ + 6.28 * X₂ – 0.9650*X₂² (9)

The regression statistics provided Multiple R 0.9962 and 0.9982; R Square 0.9981 and 0.9991 for regular and reduced model respectively.

The **3D surface graph** between surfactant concentration and homogenization speed indicated higher percentage

indicate model terms were significant. In this case, X₁, X₂, X₁X₂ and X₂² were significant model terms. given in Table 21.

Regression analysis: The effect of independent variables was evaluated using simple linear regression analysis given in Table 22. The process data was evaluated at 95% confidence interval with regular model. The process data of reduced model given in Table 23 indicated that percent process yield (Y₃) depends upon variation in surfactant concentration (X₁), homogenization speed (X₂) and square of homogenization speed (X₂)², it is defined by following equation.

yield obtained with increase in homogenization speed at different 1 – 2% surfactant concentration range. The 3D surface graph is shown in Figure 13.

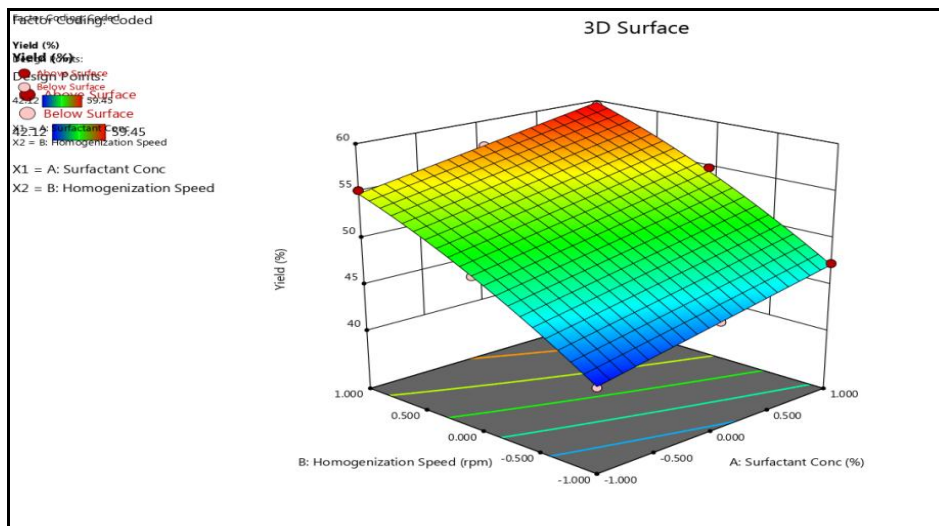


Figure 13: 3D surface graph for percent yield of nanoparticles using different different surfactant concentration and homogenization speed.

Optimization graph: The contour overlay graph for optimum desired value (yellow shaded region) gave variety of combinations to get better entrapment efficiency, better process yield and narrow particle size range. Based on optimized area through graph, following formulation and process parameters were established i.e.

surfactant concentration (2% w/v); homogenization speed (25000 rpm); chitosan concentration (0.4% w/v) and TPP concentration (0.2% w/v) to get minimum particle size along with maximum percent drug entrapment efficiency and percent process yield.

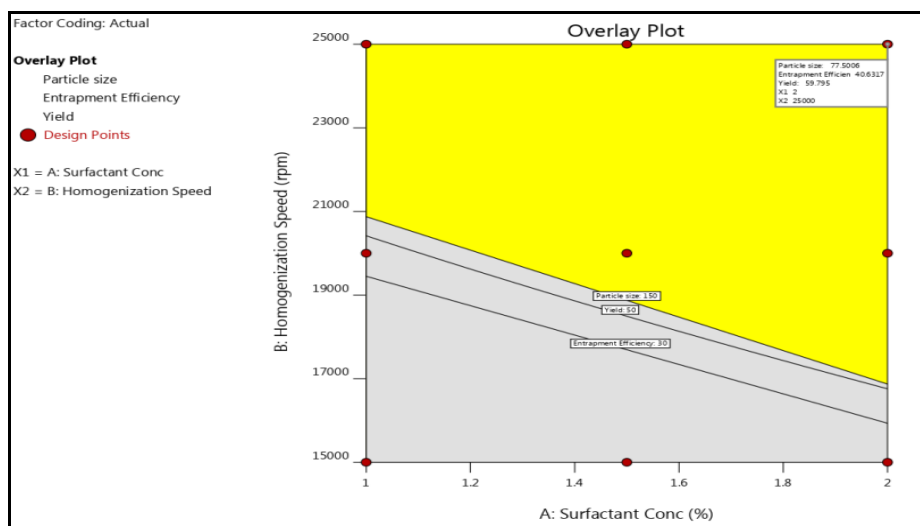


Figure 14: Contour overlay graph for optimum desired response variables for different surfactant concentrations and homogenization speeds.

Check point analysis cum optimized batch

Based on optimized area through graph, following formulation and process parameters were established i.e. surfactant concentration range (2 % v/v); homogenization speed range (25000 rpm); chitosan concentration (0.4% w/v) and TPP concentration (0.2% w/v) to get minimum mean particle size range, percent

dug entrapment efficiency (30-40%), and optimum percent yield (50-60%).

Prepared optimized batch did not show any significant difference between predicted and experimentally obtained values (Y₁: 77.08 nm, Y₂: 40.63 % and Y₃: 59.87 %). The t test was applied and p>0.05 was observed.

Table 24: Predicted and experimental response of check point cum optimized batch

Parameter	Predicted Value	Observed Value
Particle size (nm)	77.5	77.08
Entrapment efficiency (%)	40.29	40.63
Yield (%)	59.595	59.87

Evaluation of optimized batch of Felodipine nanoparticles
Particle size

Particle size of optimized formulation was found to be 77.08 which is very close to predicted value of 77.5. Hence it is confirmed that equation provided by Design Expert 10 is valid.

Z-Average (nm): 77.0784 Derived Count Rate (kcps): 94.2062301635...
 Standard Deviation: 0 Standard Deviation: 0
 %Std Deviation: 0 %Std Deviation: 0
 Variance: 0 Variance: 0

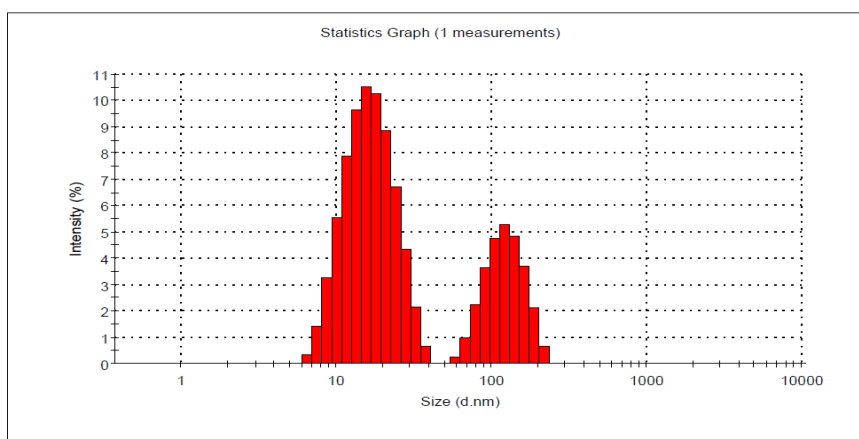


Figure 15: Particle size distribution of optimized formulation.

Zeta potential

Optimized formulation of Felodipine loaded chitosan nanoparticles was subjected to zeta potential determination. Zeta potential value of optimized formulation was found to be + 22.5 mV. This high value of zeta potential indicates that optimized formulation was stable. The magnitude of the zeta potential indicates the degree of electrostatic repulsion between adjacent,

similarly charged particles in dispersion. For very small particles, a high zeta potential will contribute to stability, i.e., the solution or dispersion will resist aggregation. When zeta potential is small, attractive forces may exceed this repulsion and the dispersion may break. Therefore, colloids having a high zeta potential (negative or positive) are electrically stabilized while colloids with low zeta potentials tend to coagulate or flocculate.

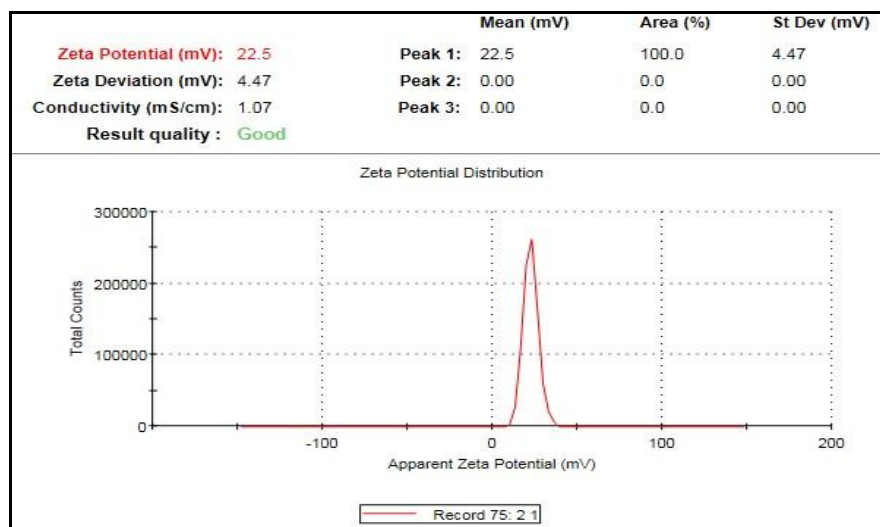


Figure 16: Zeta potential of optimized batch of Felodipine nanoparticles.

X ray diffraction

The diffraction pattern of pure Felodipine showed that drug was of crystalline nature as indicated by numerous sharp and distinct peaks at a diffraction angle of 2θ shown in Figure 17. The PXRD patterns of pure drug Felodipine has highest peak (1195) at 2θ range of 13.9, other peaks were (1086) at 2θ range of 21.7, (885) at 2θ range of 34.2 and (837) at 2θ range of 28.2. Similarly sharp crystalline peaks were also seen at a diffraction angle of 2θ in diffraction pattern of physical mixture of drug and chitosan.

The nanoparticles of optimized batch were characterized by less intensity of diffraction peaks when compared to that of pure Felodipine shown in figure 21 which demonstrates that the chemical structure of drug was not changed after preparation of nanoparticles. While optimized batch formulation has highest peak (779) at 2θ range of 6.9, other peaks were (488) at 2θ range of 14.1, (428) at 2θ range of 23.9 indicating the amorphous nature of the drug in formulation, the physical mixture has highest peak (784) at 2θ angle of 13.8, other peaks were (762) at 2θ range of 24.1, (733) at 2θ range of 26.9 indicating the reduced crystalline nature of the drug. This clearly indicates the significant reduction in crystallinity of Felodipine nanoparticles and less ordered crystals were in majority. The amorphous state would contribute to higher drug loading capacity.

It was confirmed that Felodipine existed in amorphous state in the Felodipine nanoparticles because of the

disappeared sharp peak of Felodipine in the diffraction pattern.

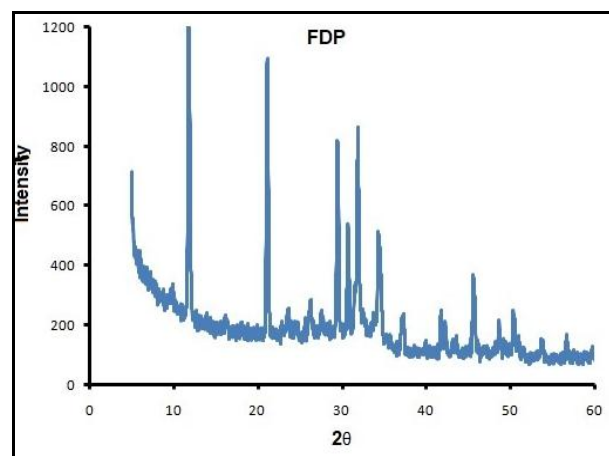


Figure 17: XRD pattern of Felodipine.

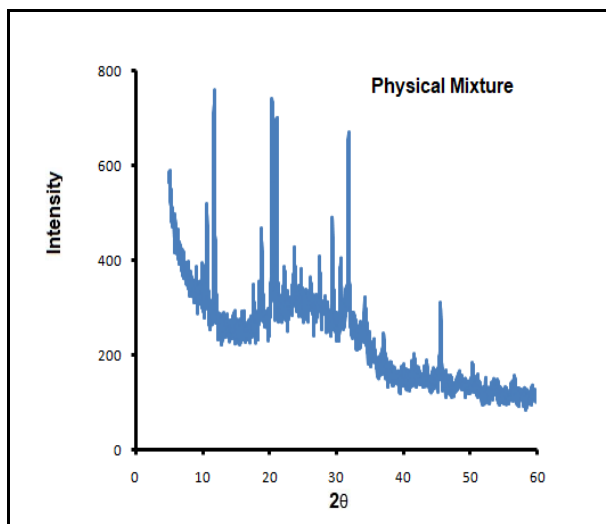


Figure 18: XRD pattern of physical mixture of Felodipine and chitosan (1:1).

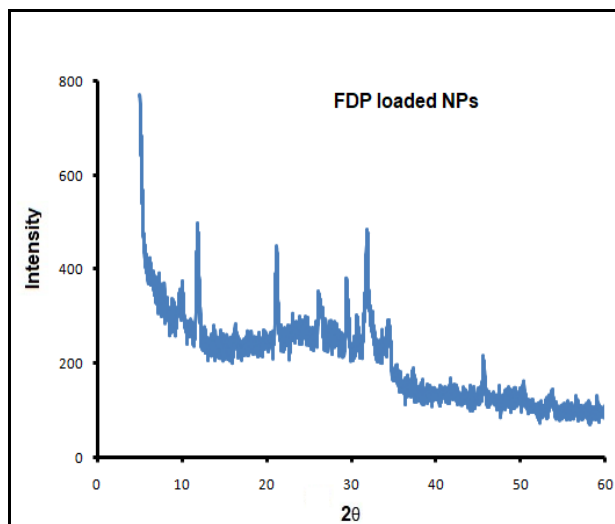


Figure 19: XRD pattern of Felodipine loaded chitosan nanoparticles.

In vitro release

In vitro release study was performed in the phosphate buffer solution (PBS) pH 6.8 containing 1% Tween 80 for the optimized batch of Felodipine loaded chitosan nanoparticles. A good released pattern was observed. Initial 32.23 ± 0.26 % drug was released in 30 minutes and 98.33 ± 0.37 % was found to be released in 3 hours.

Table 25: *In vitro* release of optimized batch of Felodipine loaded chitosan nanoparticles.

Time (min)	0	30	60	90	120	150	180
Release % \pm SD	0	32.23 ± 0.26	52.46 ± 0.63	67.74 ± 0.37	74.16 ± 0.41	86.24 ± 0.54	98.33 ± 0.37

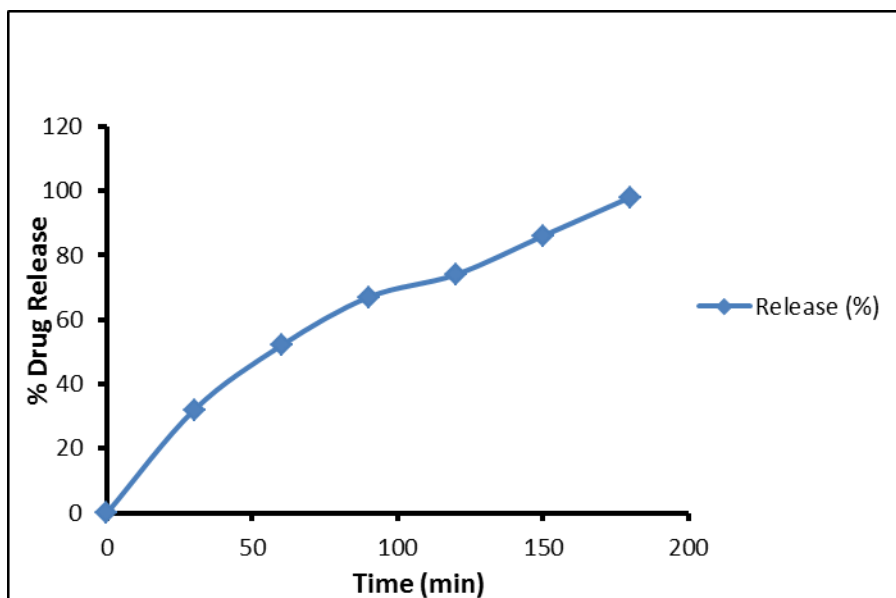


Figure 20: *In vitro* release of optimized batch of Felodipine loaded chNPs.

Transmission electron microscopy

Figure 21 shows a TEM image of Felodipine loaded chitosan nanoparticles of optimized batch. Transmission electron microscopy shows spherical particles with smooth surface. Size range in the image varies between

100 and 170 nm which is quite near to the particle size measured by zetasizer.

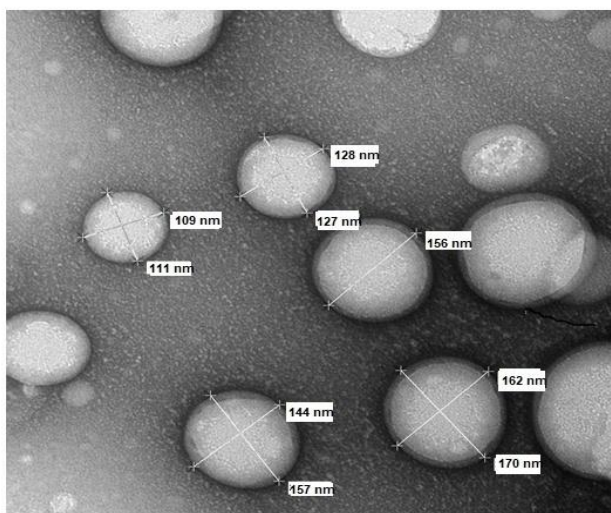


Figure 21: TEM of optimized batch of Felodipine loaded mucoadhesive chitosan nanoparticles.

CONCLUSION

The present study demonstrated the use of 3 square factorial design as an experimental design method to understand the effect of formulation and process variables in the prediction of desired responses with limited number of experiments. Although Felodipine is a poorly water soluble drug, Felodipine loaded chitosan nanoparticles were successfully prepared by using modified ionic gelation technique. Nanoparticles prepared can be used for preparing sustained release formulations. Prepared nanoparticles can also be used to prepare fast disintegrating tablets by incorporating superdisintegrants in the blend before compression.

ACKNOWLEDGEMENTS

The authors are grateful to Institute of Pharmacy, JJT University, Jhunjhunu, Rajasthan for its constant support and encouragement. We are also thankful to Hindu College of Pharmacy, Sonapat, Haryana for providing all facilities for research work.

REFERENCES

1. Jana U, Mohanty AK, Pal SL, Manna PK, Mohanta GP. Preparation and *in vitro* characterization of Felodipine loaded eudragit RS100 nanoparticles. *Int J Pharm & Pharm Sc*, 2014; 6(4): 564-567.
2. Mohanraj VJ and Chen Y. Nanoparticles – A review. *Tropical J Pharm Res*, 2006; 5(1): 561-573.
3. Couvreur P and Vauthier C. Nanotechnology: intelligent design to treat complex disease. *Pharmaceutical Research*, 2006; 23(7): 1417–1450.
4. Agnihotri SA, Mallikarjuna NN, Aminabhavi TM. Recent advances on chitosan based micro and nanoparticles in drug delivery. *Journal of Controlled Release*, 2004; 100(1): 5–28.
5. Patel BK, Parikh RH and Aboti PS. Development of oral sustained release rifampicin loaded chitosan nanoparticles by design of experiment. *Journal of Drug Delivery*, (2013) Article ID 370938, pp 1-10.

6. Arjun W, Yan S, Li G and Huili L. Preparation of aspirin and probucil in combination loaded chitosan nanoparticles and *in vitro* release study, *Carbohydrate Polymers*, 2009; 75 (4): 566-574.
7. Wang X, Chi N and Tang X. Preparation of estradiol chitosan nanoparticles for improving nasal absorption and brain targeting. *Eur J Pharmaceutics & Biopharm*, 2008; 70(3): 735-740.
8. Avadi MR, Sadeghi AMM, Mohammadpour N. (2010), Preparation and characterization of insulin nanoparticles using chitosan and arabic gum with ionic gelation method. *Nanomedicine*, 2010; 6(1): 58-63.
9. Patel R, Gajra B, Parikh RH and Patel G. Glanciclovir loaded chitosan nanoparticles: Preparation and characterization, *J Nanomed Nanotechnol*, 2016; 7(6): 1-8.
10. Yang SC, Lu L F, Ca Y, Zhu JB, Liang BW and Yang CZ. Body distribution in mice of intravenously injected camptothecin solid lipid nanoparticles and targeting effect on brain. *Journal of controlled release*, 1999; 59(3): 299-307.
11. Tamilselvan N, Raghavan CV. Formulation and characterization of Anti alzheimer's drug loaded chitosan nanoparticles and its *In vitro* biological evaluation. *Journal of Young Pharmacists*, 2015; 7(1): 28-35.
12. Mandlik SK, Nandare DS, Joshi MM, Chudiwal PD and Jain KS. Statistical and optimization of orodispersible tablets containing telmisartan using factorial design and response surface methodology. *Research Journal of Pharmacy and Technology*, 2009; 2 (3): 548-551.
13. Clavo P, Remunan-Lopez C, Vila-Jato JL and Alonso MJ. Chitosan and chitosan/ethylene oxide-propylene oxide block copolymer nanoparticles as novel carriers for proteins and vaccines. *Pharmaceutical Research*, 1997; 14(10): 1431-1436.